

Electronic Returnless Fuel System Fault Diagnosis and Isolation: A Data-Driven Approach

Bharath Pattipati¹, Krishna Pattipati¹, Youssef A. Ghoneim², Mark Howell², and Mutasim Salman²

¹*Department of Electrical and Computer Engineering
University of Connecticut
371, Fairfield Road, U-4157, Storrs, CT 06269, U.S.A
{Bharath, Krishna}@enr.uconn.edu*

²*GM Global R&D Center
30500 Mound Road
Warren, Michigan 48090, U.S.A
{youssef.ghoneim, mark.howell, mutasim.a.salman} @gm.com*

ABSTRACT

The Electronic Return-less Fuel System (ERFS) manages the delivery of fuel from the fuel tank to the engine. The pressure in the fuel line is electronically controlled by the fuel system control module by speeding up or slowing down the fuel pump. This allows the system to efficiently control the amount of fuel provided to the engine when compared to vehicles equipped with a standard fuel system wherein the fuel pump continuously runs at full speed. A failure in the fuel system that impacts the ability to deliver fuel to the engine will have an immediate effect on system performance. Consequently, improved reliability and availability, and reduction in the number of walk-home situations require efficient fault detection, isolation and prognosis of the ERFS system. This paper develops and implements data-driven fault detection, isolation and severity estimation algorithms for the ERFS. The HIL Fuel System Rig and a Chevrolet Silverado truck were used to collect and analyze the fuel system behavior under different fault conditions. Several data-driven classifiers, such as support vector machines, K-nearest Neighbor, Discriminant analysis, Bayes classifier, Partial-least squares, Quadratic and Linear classifiers, were implemented on a limited set of data for both training and testing. Regression techniques, such as Partial least squares regression and Principle component regression, are used to estimate the severity of faults. The resulting solution approach has the potential to be applicable to a wide variety of systems, ranging from automobiles to aerospace systems.

Bharath Pattipati *et. al.* This is an open-access article distributed under the terms of the Creative Commons Attribution 3.0 United States License, which permits unrestricted use, distribution, and reproduction in any medium, provided the original author and source are credited.

1. INTRODUCTION

Electronic Return-less Fuel Systems (ERFS) are fast replacing the traditional mechanical fuel delivery systems to transport fuel from the vehicle's fuel tank to the fuel rails and fuel injectors. In the ERFS system, the Fuel System Control Module (FSCM) regulates the pressure on the fuel lines to a desired pressure command from the Engine Control Module (ECM) based on the required engine speed by varying the pulse-width-modulation (PWM) control of the fuel pump. A fuel filter and a pressure regulator may be positioned on the respective intake and outlet sides of the fuel pump. Filtered fuel is thus delivered to a fuel rail, where it is ultimately injected into the engine cylinders. An ERFS includes a sealed fuel tank and lacks a dedicated fuel return line. The regulation of the fuel rate to the injectors improves the fuel economy and eliminates liquid recirculation to the fuel tank. The fuel economy is improved by reducing the electrical load on the alternator and by reducing the rail pressure under most operating conditions. With return-less systems, there is no return line and no circulation of fuel back to the fuel tank from the engine. Consequently, there is no heating of the fuel in the tank and no increase in fuel vapor pressure from driving the vehicle. This reduces the risk of excessive pressure build up inside the fuel tank, vapor leaks, and potential improvements in air/fuel ratio control, and vehicle's emission performance.

Diagnostic and prognostic methods have mainly evolved upon three major paradigms, viz., model-based (Chiang, Russel, & Braatz, 2001), data-driven, and knowledge (experience)-based approaches. The model-based approach uses a mathematical representation of the system and thus incorporates a physical understanding of the system into the monitoring scheme. A major advantage of the physics-based

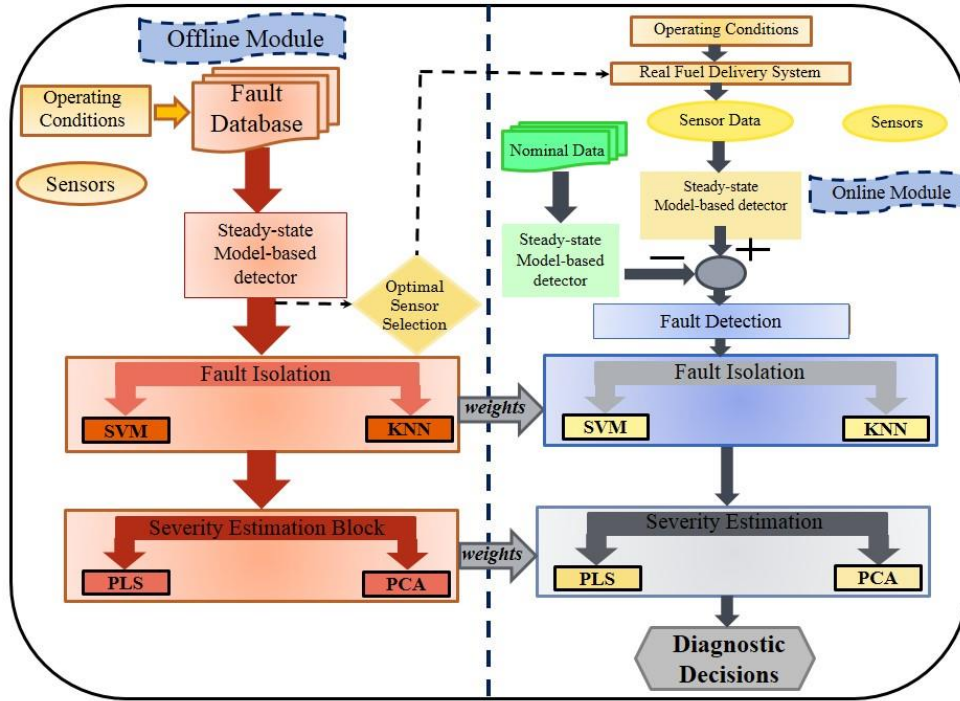


Figure 1. Framework for real-time fault detection and diagnosis of fuel systems

model is that the model bears certain behavioral resemblance to the actual system, which can be very useful in the design of a diagnostic procedure. However, models developed from

first principles are seldom used for fault diagnosis in automotive industry mainly because of their complexity. In addition, automotive system dynamics are often nonlinear,

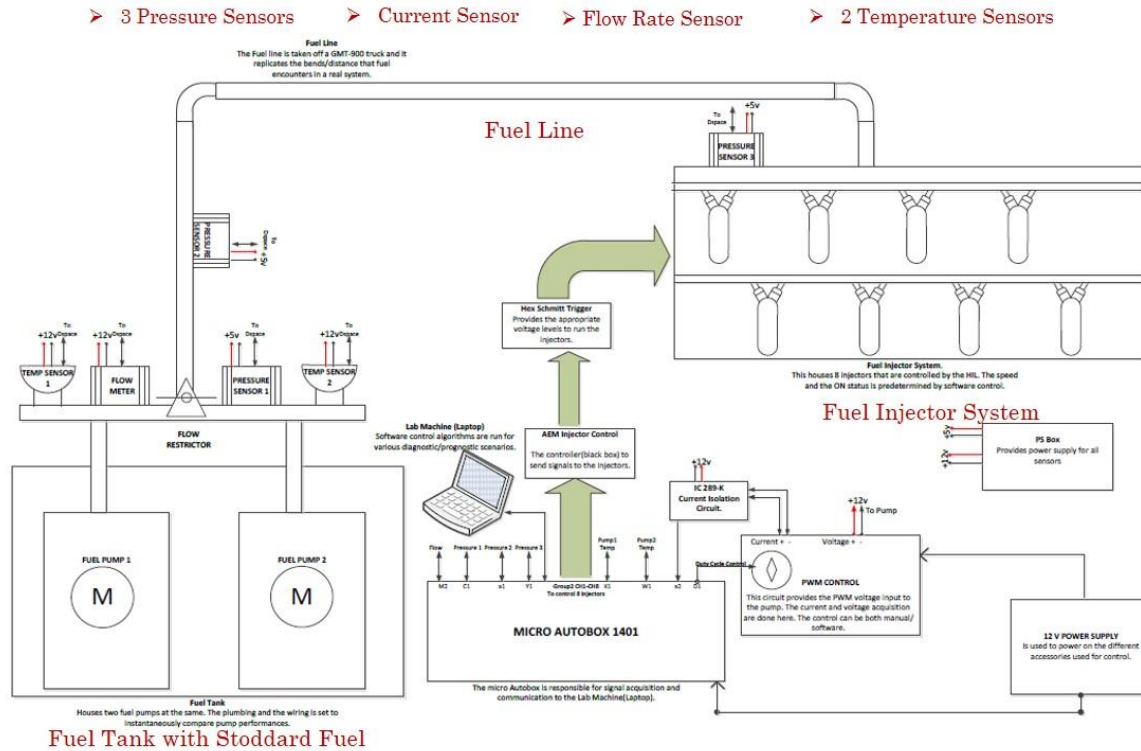


Figure 2. GMT 900 based Hardware-in-the-loop rig

which renders the design of fault diagnosis procedures difficult. However, with the advances in computing and an improved understanding of automotive systems, the design of model-based diagnosis schemes is expected to be integrated into the concurrent engineering design process. Model-based methods use statistical estimation techniques based on consistency checks (often termed residuals, “deltas”) generated using observers (e.g., Kalman filters, reduced-order unknown input observers, interacting multiple models, particle filters) and parity relations (dynamic relations among measured variables) to track the component degradations.

A data-driven approach to fault diagnosis and prognosis is preferred when system models are not available (e.g., when subsystem vendors do not share models for competitive reasons), but instead system monitoring data is available (Namburu, Azam, Luo, Choi, & Pattipati, 2007). Here, failure prognosis involves forecasting of system degradation and time-to-failure based on “state awareness” gleaned from monitored data. Neural network and statistical classification methods are illustrative of this approach. The fault scenarios must span the universe of system faults for data-driven approaches to be effective. Mathematical models may be derived (estimated or “identified”) from data as well. Data-driven models include static models and dynamic models. Static models include linear and polynomial models, and look-up tables. Dynamic models include dynamic linear and nonlinear system models.

Knowledge-based systems are based on the methods and techniques of artificial intelligence. The core components of these systems are the knowledge base and the inference mechanisms. Examples of knowledge-based systems are: rule-based systems, case-based reasoning systems, and graphical models (Luo, Tu, Pattipati, Qiao, & Chigusa, 2005). Examples of graphical models include: signed directed graphs, multi-signal flow graphs, Petri nets, and Bayesian networks (Luo et. al., 2006).

Conventional diagnostic techniques for a vehicle fuel system typically rely on knowledge of a prior failure condition. For example, when servicing a vehicle, the maintenance technician may determine that the fuel pump requires repair or replacement by direct testing and/or review of a recorded diagnostic trouble (error) code. This reactive diagnosis may not occur until vehicle performance has already been compromised. A proactive approach which tracks degradations in a fuel system is more advantageous than a reactive approach, particularly when used with emerging vehicle designs utilizing an EFRS.

In this paper, the fault detection and isolation problem of EFRS is characterized and some basic definitions are given. The main idea of fault diagnosis is to determine if there is any fault or abnormal behavior is present in the system, and to localize (isolate) the fault. In order to detect and localize the fault, a diagnosis system is needed. The diagnosis systems exploits the known signals, i.e. input signals such as control

signals, and measured output signals from the system under diagnosis, to infer the fault.

The problem of fault diagnosis can be divided into several sub-problems. Here, we focus on three:

- *Fault Detection*: To determine if a fault is present in the system and usually the time when the fault has occurred.
- *Fault Isolation*: Determination of the location of the fault, i.e. which component or components have failed.
- *Fault Severity (Estimation)*: Determination of the size and possibly time-varying behavior of a fault.

The three sub-problems are closely nested, and many algorithms cover several of them.

The focus of this paper is to develop data-driven fault isolation, and severity estimation algorithms based on neural network and statistical pattern recognition techniques exemplified by Support Vector Machines (SVM) (Vapnik, 1995), (Ge, Du, Zhang, & Xu, 2004), (Smola, Bartlett, Scholkopf, & Schuurmans, 2000), *k*-Nearest Neighbor (KNN), Principal Component Analysis (PCA) (Jackson, 1991), Partial Least Squares (PLS) (Bro, 1996), Gaussian Mixture Models (GMM), Discriminant Analysis, and so on (Bishop, 2006), (Duda, Hart, & Stork, 2001), and validate them based on fault injection in the HIL bench and the Chevrolet Silverado truck. We also estimate the severity of the isolated fault by PLS and principal component regression. The techniques chosen in the paper are based on popularity, range of complexity, robustness, data structure, and to assess the difficulty of the classification and regression problem.

The paper is organized as follows. Section 2 presents the overall framework for real-time fault detection and diagnosis of fuel delivery systems. Section 3 presents the neural network and statistical pattern recognition techniques. Section 4 presents the results of these classification and regression techniques for fault isolation and severity estimation on real data collected from the Chevrolet Silverado truck and the HIL rig. In section 5, we present the implementation of these data-driven techniques, embedded software in Simulink[®], which can be used for real-time fault isolation and severity estimation. Finally, section 6 concludes the paper with summary and future research directions.

2. FRAMEWORK FOR REAL-TIME FAULT DETECTION, ISOLATION & SEVERITY ESTIMATION OF FUEL DELIVERY SYSTEMS

The Fault Detection and Diagnosis (FDD) process consists of an *offline* training phase and an *online* testing phase. Figure 1 depicts the block diagram of a real-time FDD scheme for the fuel delivery system.

During the steady-state detection, a *model-based detector* based on residuals, parity equations, regression, and parameter estimation techniques is implemented on the ECU,

and detects the fault and estimates the state of health (SOH) during real-time operation of the vehicle. This model-based algorithm will be presented in a future paper. The nominal residuals for system operation are obtained during the offline phase via HIL rig experiments, and testing and validation is performed on the Chevrolet Silverado truck data collected at Milford Proving Grounds, and the faults detected in real-time conditions based on these nominal conditions.

In the *offline* phase, steady-state sensor data from different fault classes is used to train two fault classifiers, the Support Vector Machines (SVM), and the *k*-Nearest Neighbor (KNN). Partial Least Squares (PLS), and Principal Component Regression (PCR) estimators were also trained to assess the fault severities after fault isolation. The trained classifiers and their corresponding parameters and/or weights are exported to the online module for real-time FDD. An optimal sensor selection block is used to select the significant sensor suite for maximum diagnosability.

The *online* FDD phase consists of three steps: fault detection, fault isolation or classification, and fault identification or severity estimation. In the fault detection step, the steady-state model based detector analyses the residuals generated from the steady-state measurements of faulty and nominal systems. Upon detection of a fault, trained classifiers (SVM and KNN) are used for the online categorization of faults. In the next step, the PLS and PCA estimators corresponding to the isolated fault are used to determine its severity.

3. FAULT UNIVERSE

The fuel pump is an electronically controlled closed-loop system that maintains a desired fuel system pressure (~ 400 KPa for GMC 900 truck) and provides fuel flow on-demand to the engine under all operating conditions. The five critical fuel pump faults considered in this paper are listed in Tables 1 and 2. The faults in Table I correspond to those in GMT 900 truck and the faults in Table II are for the HIL Rig.

Altogether, fault injection experiments were performed with a commonly occurring motor/fuel pump fault, 2 sensor faults (pressure and current sensors), a pump module fault, and a fuel line fault. The fuel pressure and current sensors are located anywhere between the fuel pump and fuel rail, and the pressure and current sensor bias faults are often difficult to isolate, especially between each other, as current bias shows up as pressure bias and vice-versa. As the fuel pump degrades with age, the motor winding resistance increases and consequently, the pump PWM increases to supply the same desired pressure. A positive and negative pressure sensor bias results in the pump drawing less and more current respectively to compensate for the sensor errors. The Filter plugged fault is a result of the pump filter being blocked or clogged, and the effect of a leakage in the fuel line is represented by the fuel leakage fault.

The 2 faults in Table 1 were conducted at 2 different severity levels using a pressure and resistance box, respectively. However, since the HIL Rig allows for more flexibility, the winding fault was conducted at 10 different severity levels, and the pressure sensor bias fault, current sensor bias fault, filter plugged fault and fuel leakage faults were conducted at 4 severity levels as summarized in Table 3. The severity levels experiments of the winding fault, pressure and current sensor bias faults were conducted by adding resistances (resistance box), adding (positive) and subtracting (negative) pressure (pressure box), and injecting current, to the pump resistance, pressure, and current correspondingly. The filter plugged and fuel leakage fault experiments were conducted by restricting the fuel flow using valves (*flow restrictor* in Figure 2). The severity levels were chosen to represent the degradation of a fuel pump from low (operating normally) to high (end-of-life).

Table 1. Fault universe for GMT 900 truck

Fault	Fault Type	Component
F1.1	Pressure Sensor Bias (Slew 9.3 on pressure box)	Fuel Line
F1.2	Pressure Sensor Bias (Slew 9 on pressure box)	Fuel Line
F2.1	Winding Fault (1 Ω resistance added)	Pump/Motor
F2.2	Winding Fault (0.66 Ω resistance added)	Pump/Motor

Table 2. Fault universe for HIL rig

Fault	Fault Type	Component
F1	Winding/Commutator Fault	Pump/Motor
F2	Pressure Sensor Bias Fault	Fuel Line
F3	Current Sensor Bias Fault	Fuel Line
F4	Filter Plugged	Pump Module Fault
F5	Fuel Leakage Fault	Fuel Line

Table 3. Severity levels of each fault for HIL rig

Winding Fault	Pressure Sensor Bias Fault	Current Sensor Bias Fault	Filter Plugged	Fuel Leakage Fault
---------------	----------------------------	---------------------------	----------------	--------------------

0.3158 Ω				
0.4 Ω				
0.5 Ω			25% closed	25% closed
0.66 Ω	50 KPa	1 A	50% closed	70% closed
0.75 Ω	100 KPa	1.5 A	closed	closed
1 Ω	-50 KPa	2 A	80% closed	80% closed
1.2 Ω	-100 KPa	3 A	closed	closed
1.5 Ω			100% closed	100% closed
2 Ω				
3 Ω				

in handy to study pump dynamics. Each pump is fitted with 2 thermocouples which act as temperature sensors for monitoring the temperature and providing warning in case of overheating.

Fault simulations were run on HIL Rig using a drive profile obtained from the GMT 900 test vehicle at *Milford Proving Grounds*. A Simulink®-dSpace model of the fuel system was used to extract the sensor and parameter identifier (PID) data (current, voltage, pressure, flow, and PWM) from the HIL Rig as shown in Figure 3. The desired engine speed and pressure profiles for the Milford Proving Ground (MPG) drive cycle are presented in Figures 4 and 5, respectively.

4. FUEL DELIVERY SYSTEM HARDWARE-IN-THE-LOOP RIG

A HIL system was designed as a means for validating the diagnostic algorithms, analyze the fuel system behavior under different operating conditions, and compare the physics-based system models to the actual system. The HIL rig was controlled by a lab machine and its performance parameters were linked to a user-interface (display screen) via CAN, to warn customers of likely vehicle failure/breakdown. A schematic of the GMT 900 based HIL rig is shown in Figure 2.

The fuel tank assembly houses two pumps, one for reference (for e.g. healthy pump) and the other (e.g. faulty pump) for applying different faults and subsequently, comparing the two pumps simultaneously under various diagnostic scenarios. Each pump has its own shut-off valve, when the other pump is in operation. The entire system has a control valve that enables fuel circulation in the loop, which comes

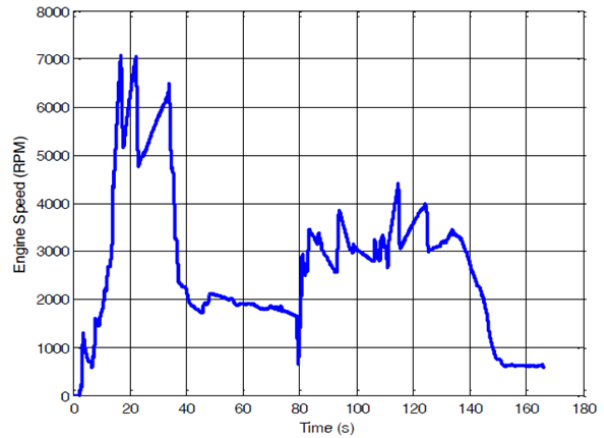


Figure 4. Desired engine speed for MPG drive cycle

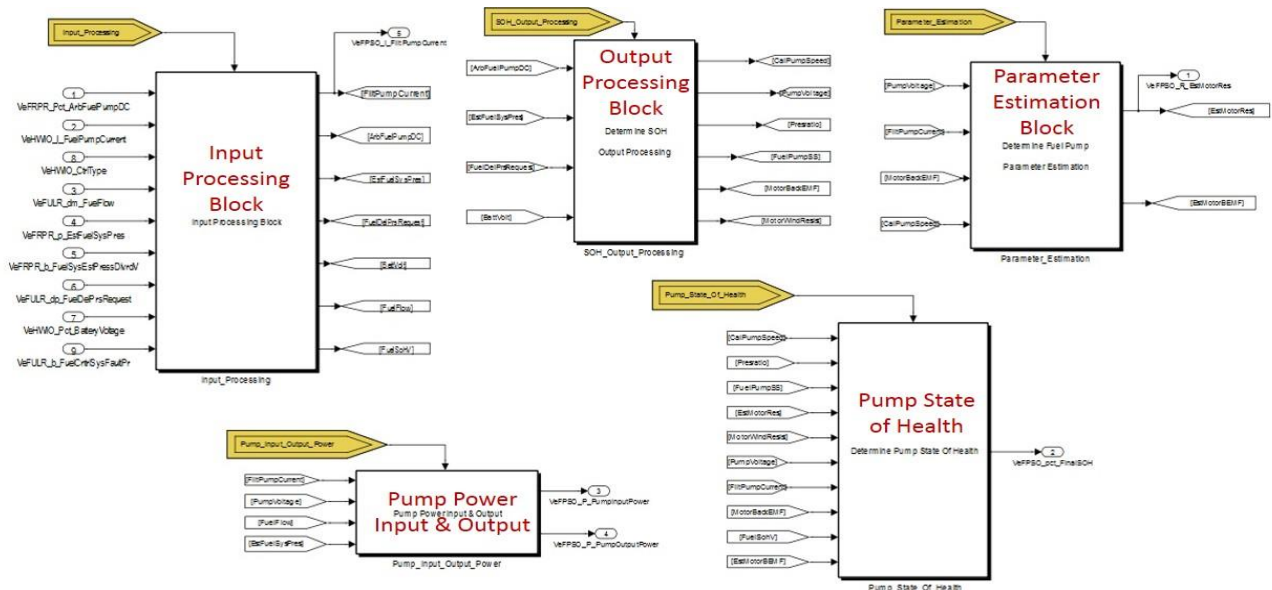


Figure 3. Simulink®-dSpace ERFs model

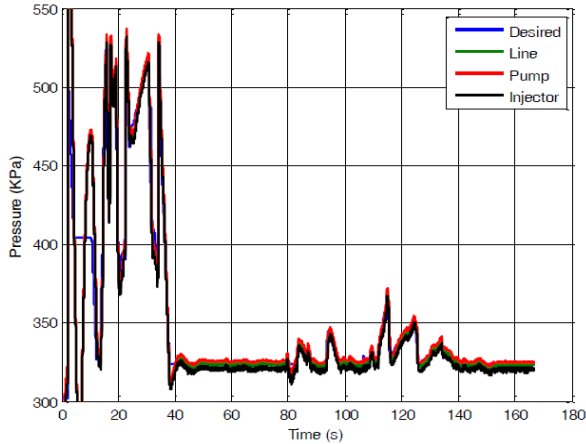


Figure 5. Desired pressure for MPG drive cycle

5. FAULT ISOLATION & SEVERITY ESTIMATION OF FUEL DELIVERY SYSTEM

5.1 Fault Isolation on the GMT 900 Truck Data

Parameter identifier (PID) data was collected from a GMT 900 (Silverado) truck under *idle* and *normal* conditions by driving on Mound Road, Warren, Michigan.

The PIDs collected are listed below.

1. Current
2. Pressure
3. Flow
4. PWM
5. Current variance
6. Desired Pressure
7. Engine Speed
8. Vehicle Speed
9. Pump Pressure
10. Pump Voltage
11. Pump Efficiency
12. Status

The *features* used for fault isolation are presented in Table 4 below.

Table 4. Features for fault isolation

Power Out (Pressure x Flow x Pump Efficiency)	Power In (Voltage x Current x PWM)	PWM	Current	Flow	Pump Pressure
---	---	-----	---------	------	------------------

The fault universe, listed in Table 1, was used to define the *fault classes* for the classification algorithms as follows:

Class 1: No Fault

Class 2: Pressure sensor bias (*Slew9.3 on the pressure box*)

Class 3: Pressure sensor bias (*Slew9 on the pressure box*)

Class 4: Winding Fault (*1 ohm resistance added*)

Class 5: Winding Fault (*0.66 ohm resistance added*)

The classification results under the two driving conditions of the truck are presented in Tables 5 and 6.

Table 5. Classification/fault isolation accuracy (5x2 cross-validation) under *idle* conditions

Rank	Classifier	Accuracy
1	SVM	100%
2	QDA	100%
3	Fisher Discriminant Analysis	1. Linear
		2. Quadratic
4	GMM	99.6747%
5	PLS	92.3520%

Table 6. Classification/fault isolation accuracy (5x2 cross-validation) under *normal driving* conditions

Rank	Classifier	Accuracy
1	QDA	99.84%
2	Fisher Discriminant Analysis	1. Linear
		2. Quadratic
3	SVM	98.2556%
4	GMM	95.1846%
5	PLS	81.2649%

The classification accuracies can be further improved using preprocessing techniques such as auto-scaling, mean-centering, PCA and PLS.

The classification task under *idle* conditions is much easier than the *normal driving* conditions. As seen in Table 5, both SVM and discriminant analysis (linear discriminant analysis and quadratic discriminant analysis) perform well while classifying faults under idling conditions (or steady-state operating conditions) of the truck. However, the classification is reasonably good even under *normal operating* conditions. SVM consistently performs well with *no false alarms* under both operating conditions of the truck and hence, was selected as one of the techniques for fault isolation in the data-driven software.

5.2 Fault Isolation and Severity Estimation on the HIL Rig Data

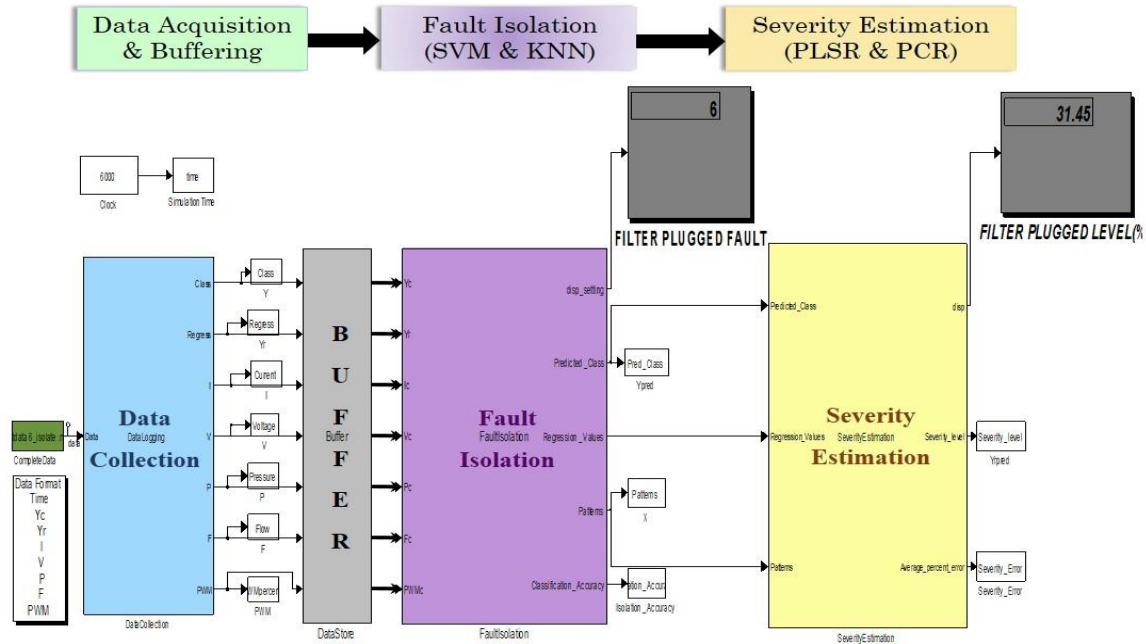


Figure 6. Data-driven fault isolation and severity estimation software

The PIDs listed below were directly used as features for the data-driven fault isolation and severity estimation.

1. Current
2. Voltage
3. Pressure
4. Flow
5. PWM

The fault classes used for isolation are as follows.

- Class 1: No Fault
- Class 2: Current Bias Fault
- Class 3: Pressure Bias Fault
- Class 4: Winding Resistance Fault
- Class 5: Fuel Leak
- Class 6: Filter Plugged

Table 7 presents the fault Isolation results for the HIL Rig. SVM, and KNN showed the highest accuracy of correct classification rate (> 99%). On the other hand, the Bayes and PLS classifiers showed the lowest accuracy.

Table 7. Classification/fault isolation accuracy (5x2 cross-validation)

Rank	Classifier	Correct Classification Rate (%)*	Overall False Alarm (%)
1	SVM	99.7028%	0.2972%
2	<i>k</i> -Nearest Neighbor		
	1. <i>k</i> =1	1. 99.5218%	1. 0.4782%
	2. <i>k</i> =2	2. 99.5218%	2. 0.4782%
	3. <i>k</i> =3	3. 99.4565%	3. 0.5435%
3	Discriminant Analysis		
	1. Linear	1. 85.2393%	1. 14.761%
	2. Diag Linear	2. 81.3819%	2. 18.618%
4	Bayes Classifier with GMM Model	82.0410%	17.959%
5	PLS	81.2871%	18.713%

1	SVM	99.7028%	0.2972%
2	<i>k</i> -Nearest Neighbor		
	1. <i>k</i> =1	1. 99.5218%	1. 0.4782%
	2. <i>k</i> =2	2. 99.5218%	2. 0.4782%
	3. <i>k</i> =3	3. 99.4565%	3. 0.5435%
3	Discriminant Analysis		
	1. Linear	1. 85.2393%	1. 14.761%
	2. Diag Linear	2. 81.3819%	2. 18.618%
4	Bayes Classifier with GMM Model	82.0410%	17.959%
5	PLS	81.2871%	18.713%

After a fault is detected and isolated, the severity estimation of the fault is needed in some cases. We used partial least squares regression (PLSR) and principal component regression (PCR) to estimate the severity of the isolated fault.

Simulations were run on the HIL Rig to collect data for each severity level. The Milford Proving Ground (MPG) drive cycle was run for each severity level of each failure model and PIDs were collected using the Simulink®-dSpace model of the ERFs system. Table 3 presented the different severity levels for each fault class.

The average percent error for each severity level is computed as follows:

$$\frac{|\text{Actual severity level} - \text{Average estimated severity level}|}{\text{Actual severity level}} \times 100 \quad (1)$$

Tables 8 and 9 show the average percent error for each severity level for both PLSR and PCR.

Table 8. Average errors for each severity level for PLSR

Winding Fault	Pressure Bias	Current Bias	Filter Plugged	Fuel Leak
8.9049%				
47.17%				
5.441%				
7.5665%	0.9262%	8.9693%	2.50146%	0.2821%
5.224%	4.2832%	3.3192%	8.25643%	0.4683%
27.978%	2.04771%	0.7428%	9.3655%	0.0952%
6.645%	0.12258%	3.5819%	11.4154%	0.1155%
16.962%				
6.55%				
15.5783%				

Table 9: Average errors for each severity level for PCR

Winding Fault	Pressure Bias	Current Bias	Filter Plugged	Fuel Leak
9.4538%				
47.4694%				
5.8208%				
7.6480%	0.8987%	8.8356%	1.7446%	0.3537%
5.43909%	4.117%	3.2657%	8.7698%	0.4622%
28.0482%	2.338%	0.5541%	9.3293%	0.1133%
6.56998%	0.4139%	3.3568%	11.6222%	0.1119%
16.864%				
6.573%				
15.5545%				

The R² results are presented in Table 10. The fit accuracy doesn't provide as good an insight into the problem of severity estimation as the average percentage errors due to the fact that it looks for strictly the same value as the truth and provides a comparison between the true (Y) and estimated values (Ŷ).

$$R^2 (\%) = \left(1 - \frac{\|Y - \hat{Y}\|_2^2}{\|Y - \text{mean}(Y)\|_2^2} \right) \times 100 \quad (2)$$

Table 10. R² fit results for different regression methods

Faults	Regression Techniques
--------	-----------------------

	PLSR	PCR
Current Bias	92.6863%	92.6285%
Pressure Bias	98.1168%	98.1251%
Winding Fault	91.9874%	91.99%
Fuel Leak	99.9035%	99.9033%
Filter Plugged	89.4918%	89.6038%

The overall data-driven fault isolation and severity estimation software based on Figure 1 was implemented in Simulink®/MATLAB® environment using Embedded MATLAB® functions as shown in Figure 6. The Data Acquisition & Buffering Block simulates real-time data storage of the sensor and PID data (current, voltage, pressure, and flow). Once a preset number of samples (e.g. 1000) are stored in the database, the fault isolation block consisting of SVM and KNN is triggered. As soon as the fault is isolated, the severity estimation block consisting of regression techniques (PLS and PCA) are triggered, and the severity level of the fault is estimated. The parameters for SVM, KNN, PLS and PCA are obtained in the training phase offline.

6. CONCLUSIONS & FUTURE WORK

In this research, a data-driven fault detection and isolation (FDI) approach for automotive ERFS is presented based on data collected from a HIL fuel system rig and a GMT 900 truck. In the Silverado truck, three fault classes (No fault, pressure bias, and resistance faults) were introduced for classification under *idle* and *normal* driving conditions. Both SVM and QDA perform with accuracies greater than 98% while classifying faults under *idle* and *normal* driving condition conditions.

In the HIL rig, six fault classes (No fault, current bias, pressure bias, motor resistance, fuel leak, and fuel filter blocked faults) were introduced under a drive profile obtained from a GMT 900 test vehicle. SVM, and KNN showed the highest accuracy of correct classification rate (> 99%). On the other hand the quadratic classifier and the linear classifier showed the lowest accuracy.

Severity estimation levels for each fault using PLSR and PCR were performed using the data from the HIL with different severity levels. The results showed that fuel leak and pressure bias fault severity estimates have the highest accuracy, while the filter plugged fault severity estimate has the lowest accuracy.

The future work will involve the following steps:

1. Extensive real-time vehicle testing to validate the robustness of the data-driven fault isolation and severity estimation approach for the ERFS.

2. Develop remaining useful life (RUL) prediction strategies for the ERFS.

3. Condition-based Maintenance (CBM) of fuel system comprising of early fault diagnosis, isolation, and RUL based on system state awareness to optimally plan and execute preventive maintenance decisions for individual and fleet of vehicles.

ACKNOWLEDGEMENT

The work reported in this paper was supported by National science foundation (NSF) under grants ECCS-0931956 (NSF CPS) and ECCS-1001445 (NSF GOALI). We thank GM R&D and NSF for their support of this work. Any opinions expressed in this paper are solely those of the authors and do not represent those of the sponsor.

The authors would like to express their gratitude to Mehmet E. Inan for his help in data collection and analysis.

The authors thank the anonymous reviewers for valuable suggestions that enhanced the paper.

REFERENCES

- Bishop, C.M. (2006). *Pattern Recognition and Machine Learning*. New York, USA: Springer.
- Bro, R. (1996). Multiway Calibration. *Multilinear PLS. Journal of Chemometrics*, vol.10, issue 1, pp. 47-61. doi: 10.1002/(SICI)1099-128X(199601)10:1<47::AID-CEM400>3.0.CO;2-C
- Chiang, L. H., Russel, E., & Braatz, R. (2001). *Fault Detection and Diagnosis in Industrial Systems*. London, U.K.: Springer-Verlag.
- Duda, R. O., Hart, P. E., & Stork, D. G. (2001). *Pattern Classification*. 2nd edition, New York, USA: John Wiley and Sons.
- Ge, M., Du, R., Zhang, G., & Xu, Y. (2004). Fault diagnosis using support vector machine with an application in sheet metal stamping operations. *Mechanical Systems and Signal Processing*, vol. 18, pp.143-159. doi: 10.1016/S0888-3270(03)00071-2
- Jackson, J. E. (1991). *A User's Guide to Principal Components*. New York, USA: John Wiley & Sons.
- Luo, J., Tu, H., Pattipati, K., Qiao, L., & Chigusa, S. (2005). Graphical models for diagnosis knowledge representation and inference. *IEEE Autotestcon*, pp. 483-489. doi: 10.1109/MIM.2006.1664042
- Luo, J., Tu, H., Pattipati, K., Qiao, L., & Chigusa, S. (2006). Diagnosis knowledge representation and inference. *IEEE Instrumentation and Measurement Magazine*, vol. 9, issue 4, pp. 45-52. doi: 10.1109/MIM.2006.1664042
- Namburu, S. M., Azam, M. S., Luo, J., Choi, K., & Pattipati, K. R. (2007). Data-driven modeling, fault diagnosis, and optimal sensor selection for HVAC chillers. *IEEE*

transactions on automation science and engineering, vol. 4, no. 3. doi: 10.1109/TASE.2006.888053

Smola, A. J., Bartlett, P. L., Scholkopf, B., & Schuurmans, D. (2000). *Advances in Large Margin Classifiers*. Cambridge, Massachusetts: The MIT Press.

Vapnik, V. (1995). *The Nature of Statistical Learning Theory*. New York, USA: Springer.